Rochester Institute of Technology

RIT Digital Institutional Repository

Presentations and other scholarship

Faculty & Staff Scholarship

5-12-2005

25nm Immersion Lithography at a 193nm Wavelength

Bruce W. Smith
Rochester Institute of Technology

Yongfa Fan
Rochester Institute of Technology

Michael Slocum
Rochester Institute of Technology

Lena Zavyalova
Rochester Institute of Technology

Follow this and additional works at: https://repository.rit.edu/other

Recommended Citation

Bruce W. Smith, Yongfa Fan, Michael Slocum, Lena Zavyalova, "25 nm immersion lithography at 193 nm wavelength", Proc. SPIE 5754, Optical Microlithography XVIII, (12 May 2004); doi: 10.1117/12.602414; https://doi.org/10.1117/12.602414

This Conference Paper is brought to you for free and open access by the RIT Libraries. For more information, please contact repository@rit.edu.

25nm Immersion Lithography at a 193nm Wavelength

Bruce W. Smith, Yongfa Fan, Michael Slocum, Lena Zavyalova

Rochester Institute of Technology, Microelectronic Engineering Department, 82 Lomb Memorial Drive, Rochester, New York 14623
Amphibian Systems, 125 Tech Park Drive, Rochester, New York 14623

ABSTRACT

The physical limitations of lithographic imaging are ultimately imposed by the refractive indices of the materials involved. At oblique collection angles, the numerical aperture of an optical system is determined by $n\sin(\theta)$, where n is the lowest material refractive index (in the absence of any refractive power through curvature). For 193nm water immersion lithography, the fluid is the limiting material, with a refractive index of near 1.44, followed by the lens material (if planar) with a refractive index near 1.56, and the photoresist, with a refractive index near 1.75. A critical goal for immersion imaging improvement is to first increase the refractive indices of the weakest link, namely the fluid or the lens material. This paper will present an approach to immersion lithography that will allow for the exploration into the extreme limits of immersion lithography by eliminating the fluid altogether. By using a solid immersion lithography (SIL) approach, we have developed a method to contact the last element of an imaging system directly to the photoresist. Furthermore, by fabricating this last element as an aluminum oxide (sapphire) prism, we can increase its refractive index to a value near 1.92. The photoresist becomes the material with the lowest refractive index and imaging becomes possible down to 28nm for a resist index of 1.75 (and 25nm for a photoresist with a refractive index of 1.93). Imaging is based on two-beam Talbot interference of a phase grating mask, illuminated with highly polarized 193nm ArF radiation. Additionally, a roadmap is presented to show the possible extension of 193nm lithography to the year 2020.

Keywords: Immersion, Lithography, Solid Immersion, ArF, Excimer Laser

1. INTRODUCTION

By replacing the air gap between the bottom lens element and the photoresist film of a photolithographic imaging system with a fluid, numerical apertures above 1.0 are possible. Immersion lithography is thus best viewed as an enabling technology for hyper-NA imaging. The real challenges of immersion lithography are not the fluid mechanics issues addressed in the initial stages of the technology but instead the problems associated with very large angles, and associated polarization, reflection and refraction effects.

Hyper-NA lithography is generally considered to be imaging with angles close to 90° in any media within an imaging system to achieve numerical apertures above 1.0 The optical invariant $NA = n_i \sin\theta$ implies that the increases in numerical aperture for large angles is accomplished mainly with increases in refractive index, since the increase in the corresponding sine function increases quite slowly. The sine of 68° is 0.93 and a 20° increase to 88º leads to a gain in numerical aperture of merely 7.5%. Increasing the propagation angle within a lens system above 68° is therefore not significantly beneficial and not a part most current lens system designs. Hyper NA is therefore forced upon material refractive index, where the media with the lowest index provides a “weak link” to refractive power. The current situation is one where the photoresist possesses the highest refractive index and a photoresist top-coat has the lowest refractive index where:

$$n_{PR} > n_{glass} > n_{fluid} > n_{top\text{-}coat}$$

The ultimate resolution of a lithography tool therefore becomes a function of the lowest refractive index. Methods are already being employed in lithography to achieve k_1 process factors near 0.30, where 0.25 is the physical limit. It is therefore not likely that much further ground will be achieved as we move into hyper NA immersion lithography.

Optical Microlithography XVIII, edited by Bruce W. Smith,
Proceedings of SPIE Vol. 5754 (SPIE, Bellingham, WA, 2005)
0277-786X/05/$15 · doi: 10.1117/12.602414

The minimum half-pitch (hp) for 193nm lithography following classical optical scaling for a 68° propagation angle becomes:

$$hp_{\min} = \frac{k_1 \lambda}{n_i \sin\theta} = \frac{(0.25\ to\ 0.30)(193)}{n_i (0.93)} = \frac{52}{n_i}\ to\ \frac{62}{n_i} \quad nm$$

for k_1 values between 0.25 and 0.30.

2. HIGH INDEX IMEMRSION FLUIDS

An accompanying paper describes the challenges of the identification and measurement of imaging fluids with refractive index values greater than that of water [1]. Figure 1 shows a plot of for three example fluids (along with water) for wavelengths between 190 and 290nm. These fluids and their optical properties (n,k) are:

Fluid	**(n,k)**
Aluminum chloride, AlCl3	($1.60, 10^{-4}$)
Hydrogen phosphate, H_3PO4	($1.54, 10^{-5}$)
Sodium sulfate, Na_2SO_4	($1.49, 10^{-4}$)
Water	($1.44, 10^{-6}$)

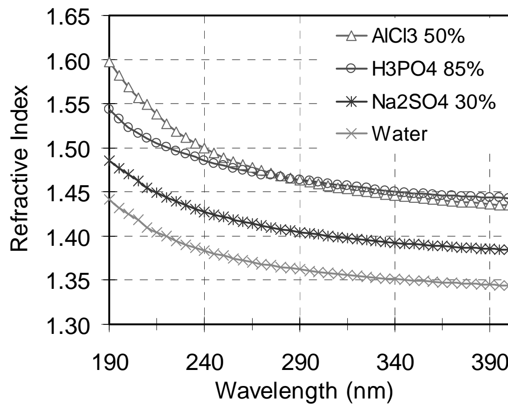

Figure 1. Refractive index vs. wavelength for four immersion lithography fluids.

The absorption of these fluids (proportional to the extinction coefficient, or $4\pi k/\lambda$) is larger than water by one order of magnitude (for hydrogen phosphate) and two orders of magnitude (for aluminum chloride and sodium sulfate), but it is expected that these values can be decreased somewhat with the use of more purified materials. Imaging has been carried out with each of these fluids, as shown in Figure 2.

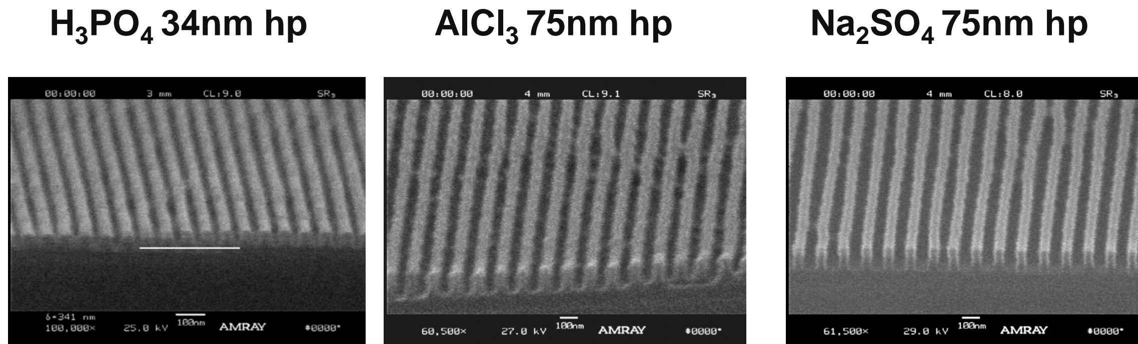

Figure 2. Lithographic imaging using high index inorganic fluids.

3. MATERIAL LIMITS

Total internal reflection can be calculated from Snell's law for angles above a critical angle:

$$\theta c = \sin^{-1}(n_L/n_H)$$

where n_H and n_L are low and high refractive index media respectively. Figure 3 is a plot of the reflectance at the glass/media interface for an optical system using a planar fused silica last element. Both TE and TM polarization are plotted for air, water, a high index fluid (HIF, assumed here to have an index of 1.54), and solid immersion lithography (SIL, where no interfacial media exists between the lens and the photoresist media). The limiting resolution for these situations becomes:

$$hp_{\text{water}} = 36 \text{ to } 43\text{nm}$$
$$hp_{\text{HIF-1.54}} = 33 \text{ to } 40\text{nm}$$
$$hp_{\text{SIL-1.56}} = 33 \text{ to } 40\text{nm}$$

showing that solid immersion shows no benefit over HIF imaging when the refractive index of the optical material is not sufficiently greater than the refractive index of the fluid media. The images in Figure 4 demonstrate these limits, where 32nm hp is achieved at 1.50NA and 31nm hp is achieved at 1.54NA (which is nearly 90° in the HIF fluid used). A Talbot immersion interference lithography setup has been employed to achieve these results. The system description has been presented earlier [2]. The setup is shown in Figure 5.

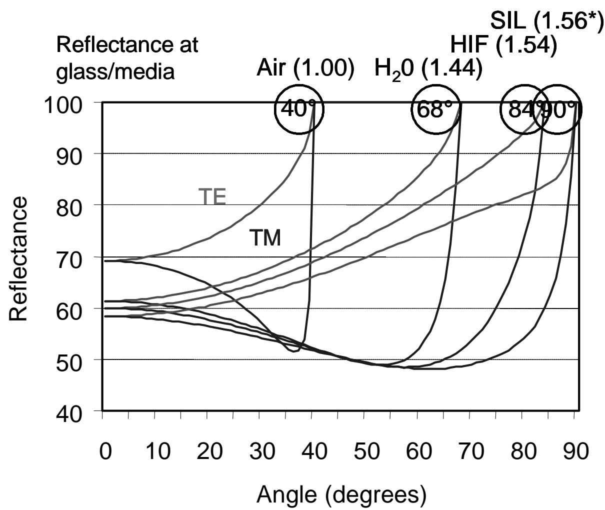

Figure 3. Reflectance at glass/media interfaces for various materials.

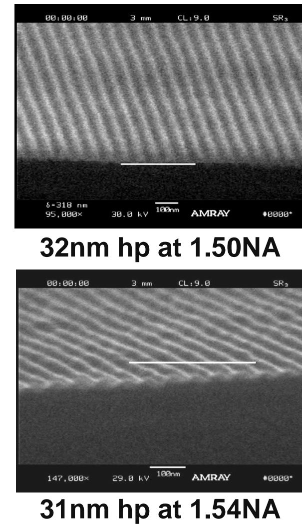

Figure 4. 32 and 31nm half-pitch imaging.

Figure 5. Talbot immersion interference imaging setup.

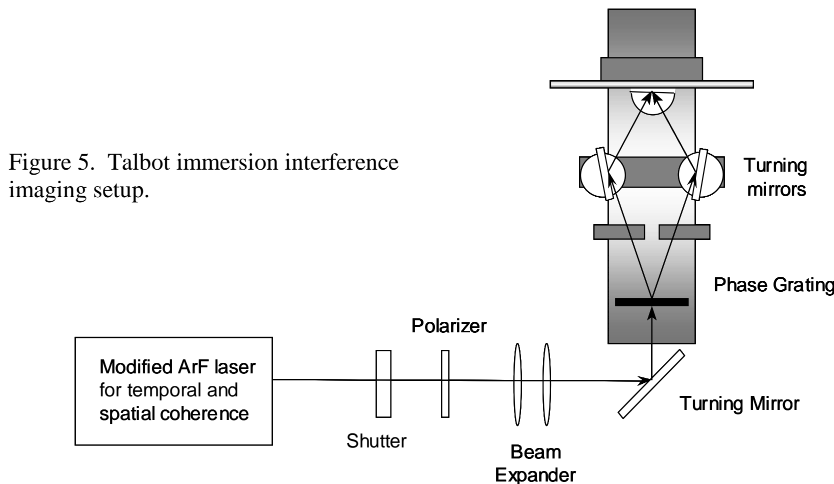

The refractive power of the optics in a lithography tool can be increased in two ways, as depicted in Figure 6. One method, shown in Figure 6a is through the increase in refractive index of the material. This might be accomplished if suitable dopants to fused silica can be identified which do not adversely impact the absorption, mechanical, thermal, or chemical properties of the material. A 10% increase in refractive index may allow for values up to 1.72. No suitable additives have been identified at this time however. Another alternative is the use of other oxides, such as aluminum oxide (sapphire, Al_2O_3). Sapphire has a refractive index of 1.92 at 193nm but is a hexagonal crystal and highly birefrigent. Its hardness also presents problems with polishing to meet strict optical requirements. A planar surface of sapphire is possible, however, allowing for opportunities for application as last-element material. A second method that can be employed to increase the refractive power of a glass element is through surface curvature, as shown in Figure 6b. Issues involved with this scenario include a variation in optical path length across the optical field (though this could be used as an advantage) and filling and trapping issues with fluid filling. New lens designs may begin to take advantage of non-planar surfaces to reduce the requirements on material index.

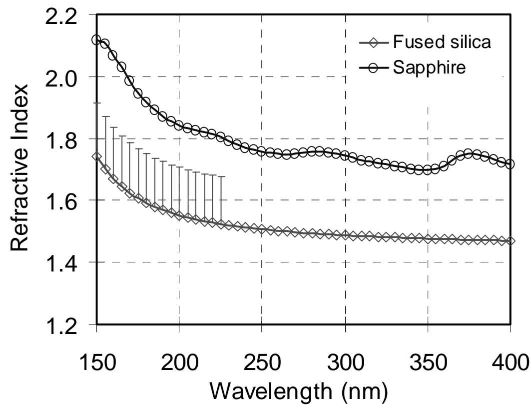

Figure 6a. Sapphire and modified fused silica for increased refractive index.

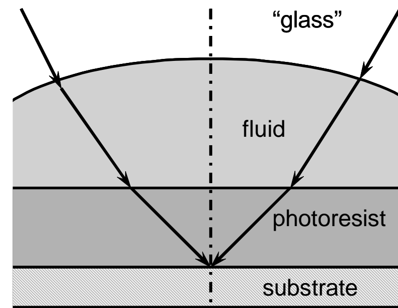

Figure 6b. Element curvature for increased refractive index.

4. NEAR FIELD COUPLING AND SOLID IMEMRSION

The previous discussions suggest the "weak link" approach to addressing hyper-NA, where the media of lowest refractive index needs to be modified or replaced. A geometrical approach to describing the situation may not be adequate however and Snell's law doesn't necessarily drive the limitations. This becomes increasingly important when considering the film stack requirements for 32nm half-pitch resolution and below. For photoresist films corresponding to 1:1.5 to 1:2 aspect ratios, layers between 48 and 64nm thick are likely. The optical thickness of such layers is 0.4 to 0.6 waves at normal incidence, 0.55 to 0.85 waves at 45° in the film (or 1.2NA), and 0.8 to 1.2 waves at 60 ° in the film (or 1.5NA). Furthermore, a top-coat at a thickness of 20-60nm is likely. Wave propagation in such thin films does not follow conventional far field description. Instead, the evanescent TIR field propagates in the near field with some degree of spatial information.

The role of propagating and evanescent waves in solid immersion lens system has been described previously [3]. Figure 7 depicts the coupling of wavefronts directed toward an interface between two media, where the lower media has a lower refractive index. The propagating wavefronts at angles below TIR are transmitted uniformly while the coupling of wavefronts in the evanescent region at angles above TIR is inhomogeneous. The result is an effect of spatial filtering for the evanescent field which follows an exponential decay associated with the difference in refractive index at the media interface and the incoming propagation angle. When combined with the absorption losses within the lower media, the energy coupled into a thin layer becomes:

$$A(z) = e^{-\left(\frac{2\pi n_{upper}}{\lambda}\left[\sin^2\theta - \left(\frac{n_{lower}}{n_{upper}}\right)^2\right]^{1/2} + \alpha\right)z}$$

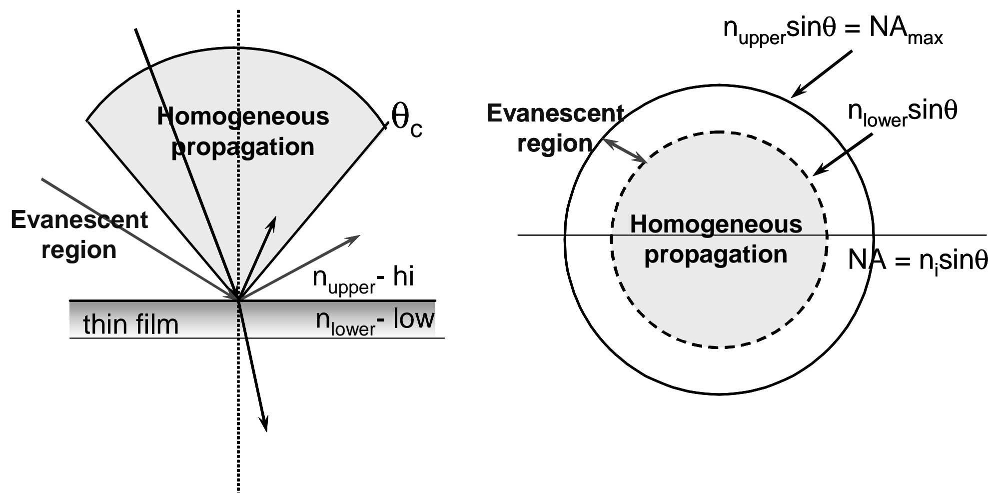

Figure 7. Homogeneous and evanescent wave coupling into thin films.

Figure 8 shows the impact that this effect would have on a typical 32nm half-pitch lithography condition, where a propagation angle of 81° is considered in a 1.54 index HIF (hydrogen phosphate) above a resist top-coat layer with a refractive index of 1.40. TIR occurs at 63.8°, substantially lower than the angle considered. If zero absorbance in the top-coat layer is assumed, the energy coupled through the film for this case becomes $A(z) = e^{-0.019z}$. Figure 9 shows experimental verification of this result using a calculation of the near field effects from ILSim, a vector immersion interference lithography simulator [4]. Three top coat film thicknesses are shown, 18nm, 40nm, and 56nm. The image intensity for the 31nm features decreases with increasing film thickness and, in the presence of non-zero background intensity (from flare for instance), modulation also decreases. The 18nm film thickness result shows image degradation from chemical contamination as the top coat layer is not sufficient to protect the photoresist from environmental contamination. There are several implications from this result. First, the requirements of a thin film top-coat are reduced as the refractive index can be lower than the fluid/resist index. Higher index photoresists than those currently available may not be necessary. A thin fluid layer could have a lower refractive index than the glass. SIL may be feasible if small fluid gaps can be maintained. And lastly, SIL can be useful to evaluate the imaging limits of photoresist. These consequences of course need to accommodate the loss in the evanescent near-field energy through the entire film stack.

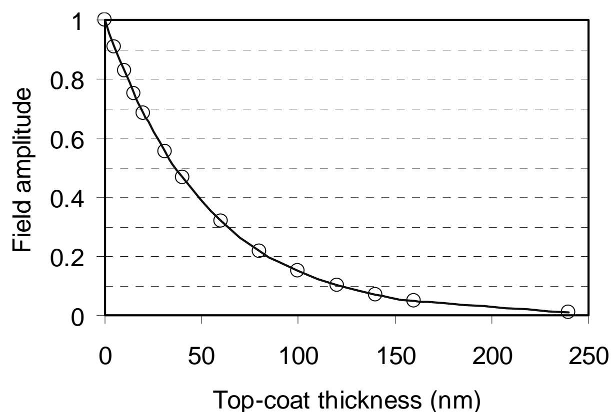

Figure 8. The decay of evanescent energy coupled into a photoresist film stack for 32nm half-pitch imaging.

5. SOLID IMMERSION LITHOGRAPHY USING SAPPHIRE

Figure 10 shows the reflectance at the imaging interface for an optical system using a sapphire as last element. Both TE and TM polarization are plotted for air, water, a high index fluid, and solid immersion. In this case, the refractive index of sapphire (1.92) moves the photoresist to having the lowest refractive index for solid immersion, where a numerical aperture as large as 1.76 (the assumed refractive index of the photoresist) results. Figure 11 is an experimental setup for

such a scenario, where a hexagonal, single-crystalline equilateral prism is used with Talbot interference immersion imaging. The numerical aperture of the prism at 60° is 1.67 but the system can accommodate an NA value up to 1.81 at a 70° propagation angle. The birefringence of sapphire at 193nm is $8x10^{-3}$ but does not impact imaging in one direction using linear polarization. Magnesium fluoride is used as an AR layer, providing near zero reflectivity across the targeted range of angles. The current challenges with the system are dominated by the photoresist film stack, where materials capable of sub-30nm resolution are being pursued along with multilayer bottom anti-reflective coatings (BARCs) to suppress reflection at these extreme angles.

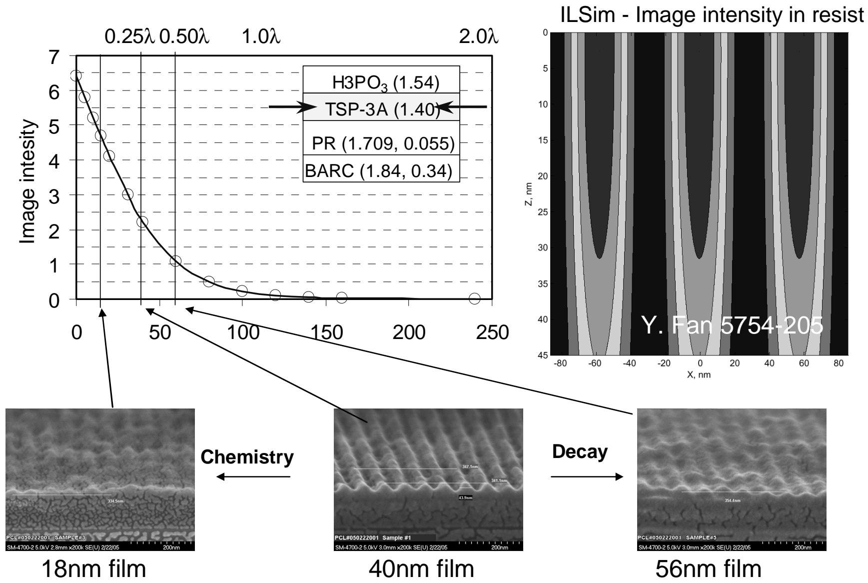

Figure 9. Lithographic imaging into a top-coat with a refractive index below the numerical aperture of the imaging system.

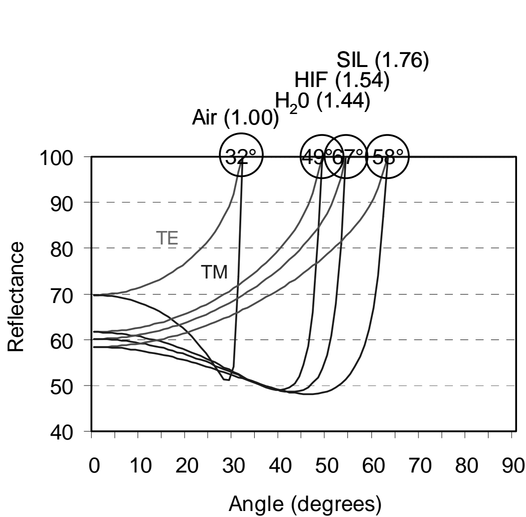

Figure 10. Reflectance at sapphire/media interfaces for various materials.

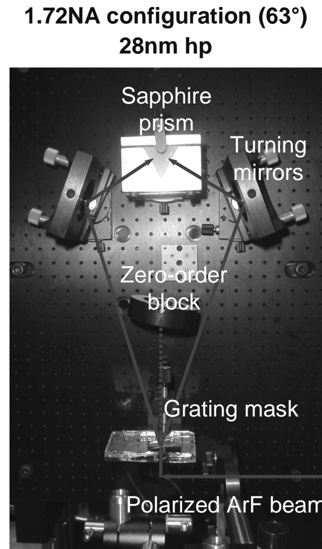

Figure 11. Experimental setup for sapphire SIL at 1.72NA.

6. CONCLUSIONS - THE 30 YEAR 193nm ROADMAP

Lithography at 193nm using the ArF excimer began in the early 1990's in development groups at IBM, MIT- Lincoln Laboratories, and the Rochester Institute of Technology. Water immersion lithography can be expected to extend the lifetime of 193nm technology into sub-32nm generations through the development of new processes and materials. Figure 12 shows a roadmap for 193nm lithography that can be projected to allow imaging down to 25nm half pitch. This will require the development of high index fluids with refractive indices of 1.54 (HIF-1), 1.65-1.70 (HIF-2), high index glass (>1.56), and high index photoresist (1.8-1.93). The limit of 25nm can be projected if no index less than 1.93 is assumed, or if the last glass surface of the optical system in not planar. SIL of course becomes difficult with non-planar surfaces. Minimum half-pitch resolution becomes 0.25 λ/NA or 25nm. It is anticipated that demonstration of 25nm imaging can be carried out in an interferometry mode. Whether this can be extended to real manufacturable lithography will have to be seen.

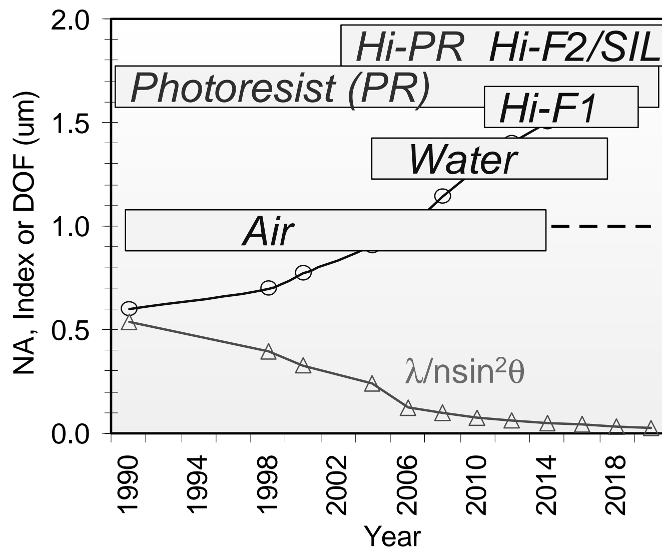

Figure 12. The 30-year 193nm lithography roadmap.

7. REFERENCES

[1] J. Zhou, Y. Fan, A. Bourov, L. Zavyalova, A. Estroff, N. Lafferty, B. Smith, "Immersion Lithography Fluids for High NA 193nm lithography, " Proc. SPIE 5754 (2005)

[2] B.W. Smith, A. Bourov, Y. Fan, L. Zavyalova, N. Lafferty, F. Cropanese, 'Approaching the numerical aperture of water - Immersion lithography at 193nm," Proc. SPIE 5377 (2004).

[3] T.D. Milster, J.S. Jo, K. Hirota, "Roles of propagating and evanescent waves in solid immersion lens system," Appl. Opt., Vol. 38, No. 23, 1999, 5046.

[4] Y. Fan, A. Bourov, L. Zavyalova, J. Zhou, A. Estroff, N. Lafferty, B.W. Smith, "ILSim – A compact simulation tool for interferometric lithography, " Proc. SPIE 5754 (2005).